RSC Advances

ROYAL SOCIETY OF CHEMISTRY

www.rsc.org/advances

Phase separation in PSf/DMF/water system: A proposed mechanism for macrovoid formation

Lei Yu, Feng Yang *, Ming Xiang

State Key Laboratory of Polymer Materials Engineering, Polymer Research Institute of Sichuan University, Chengdu 610065, People's Republic of China

*Corresponding authors' e-mail addresses: yangfengscu@126.com (Feng Yang); tel.: +86-028-8540 5347, fax: +86-028-8540 6578.

Abstract

Formation of polysulfone (PSf) membranes from PSf/ N,N-dimethylformamide (DMF)/water system was studied with optical microscopic observation. Visualization of phase separation process was performed and immersion precipitated membranes were prepared with polymer solution containing different PSf concentration and coagulation bath having variable DMF content. Diffusion rate of water into polymer solution was found to be reduced with increasing PSf concentration in polymer solution or DMF content in coagulation bath. Scanning electron microscope (SEM) images of hand casted membranes showed unique occurrence of macrovoid and based on the optical microscopic findings, a mechanism for macrovoid formation was proposed. The contraction of bi-continuous phase separated network of polymer rich phase might cause inflow of polymer lean phase, leading to the formation of a polymer lean layer at the phase separating boundary, which should be responsible for macrovoid formation. The occurrence of macrovoid was furtherly related to the resistance to compaction of immersion precipitated membranes. Results from compression test indicated that the membrane is mechanically more sustainable with damping of macrovoid.

Key words

Polysulfone, phase separation, membrane, macrovoid, bi-continuous

1. Introduction

Since its first introduction to industrial preparation of polymeric membranes by Loeb and Sourirajan [1], the phase inversion process has long been a research focus and a plethora of knowledge has been generated about this process. Many ways can lead to the phase inversion of a polymer solution, such as solvent evaporation or controlled evaporation, vapor-induced precipitation, thermal precipitation, and immersion precipitation [2]. Of all these techniques, immersion precipitation is the most popular one. Generally, a dope polymer solution which consists a polymer, a solvent, and additives is firstly coated on a mechanical support or extruded through an annular spinneret, and subsequently immersed into a coagulation bath to let the polymer solidify by exchange of the solvent and non-solvent. The membrane structure is thus obtained by solidification of the phase-separated polymer rich phase to form the skeleton structure and the extraction of the phase-separated polymer lean phase to form the cavity [3]. During immersion precipitation, the phase separation process usually involves a polymer,a solvent, and a non-solvent. This typical tri-component system can be simplified as polymer/solvent/non-solvent system.

Polysulfone (PSf), having beening commercially used for quite some time, is one of the most common polymers used to make membranes by phase inversion process. Its commercial availability, favorable selectivity-permeability characteristics, mechanical and thermal stability, as well as chemical resistivity in acidic and alkaline media have made this material superior for

preparing the support layer of thin film composite (TFC) membrane [3-13]. N,N-dimethylformamide (DMF) is among the most frequently used solvents for making support layer with PSf because of its low cost and the appropriate mutual affinity between DMF and water. Membranes made from PSf/DMF/water system often show a damped and unique occurrence of macrovoids. They are expected mechanically more resistant to external forces [14]. Therefore, this kind of membrane finds its ideal application in TFC membrane used for seawater reverse osmosis (SWRO) desalination where high pressure (about 60 bar) is usually employed [15, 16]. Still, there are only limited researches dealing with the membranes prepared from phase inversion process in PSf/DMF/water system [17-25]. Furthermore, the formation mechanism of the derived membrane structure is not so clear and lacks of theoretical support.

Upon phase inversion, the cross-section of a membrane ordinarily exhibits a microstructure that contains the denser skin layer and the more porous sublayer. They are hypothesized to be formed by two separate [26-28] mechanisms: the dense skin layer is formed by gelation of the abruptly concentrated polymer solution at the surface of the dope solution when contacted with the coagulation bath; the porous sublayer with graded structures underneath the skin layer is formed by liquid–liquid demixing and the competition process between coarsening of the polymer lean phase and gelation of the polymer rich phase. The theoretically unfavored spinodal decomposition with the fast composition change can also occur if the time that the solution stays in the meta-stable region is short enough [29-31]. Kuo et al. [32] observed that during vapor induced phase separation (VIPS), the nascent bi-continuous structure can be formed by spinodal decomposition and coarsened to cellular pores when solvent of low volatility was adopted. Tsai et al. [33] found that the nascent bi-continuous structure, formed by VIPS of PSf solution, could be effectively retained

when 2-pyrrolidinone was employed as the solvent whose viscosity is substantially high (13.3 cp at 25 °C). The theoretically calculated phase diagram of PSf/DMF/water system by Barth et al. [18] showed a narrow homogeneous region and large spinodal decomposition region, which implies that the polymer solution can be able to rapidly cross the meta-stable region without phase separation and reaches the unstable region to go through spinodal decomposition [31]. The derived bi-continuous structure of the sublayer is attractive for SWRO desalination as high water flux can be achieved without decreasing the salt rejection substantially.

The formation of membrane structure is usually characterized by the occurrence of macrovoids which is a nuisance in the case of membranes intended for reverse osmosis application and always attracts attention from membranologists. Empirical rules for controlling the formation of macrovoids were found two decades ago by Smolders et al. [34]: (i) macrovoids are formed in case of instantaneous demixing except when the polymer concentration and/or the non-solvent concentration in the casting solution exceed a minimum value; (ii) macrovoids are damped by delayed demixing, except when the delay time is very short. A number of hypotheses have been made based primarily on optical microscopy and scanning electron microscopy (SEM) as well as theoretical computation to elucidate their formation mechanism [30, 34-49], among which the one proposed by Smolders et al. [34] is the most classical. They claimed that macrovoids are initiated by freshly formed nuclei of the diluted phase when a change in precipitation conditions from instantaneous to delayed onset of demixing occurs at a certain distance from the film interface. Diffusion of solvent expelled from the surrounding polymer solution causes macrovoid growth. Smolders' group correctly argued that macrovoid formation and growth requires instantaneous rather than delayed demixing. However, it is now generally recognized that this is an 'effect'

rather than a 'cause' for macrovoid formation and growth. Khare et al. [42] and Pekny et al. [43] advanced the hypothesis that macrovoid formation and growth requires the presence of a supersaturated region in advance of the macrovoid front. Lee et al. [44] developed a detailed mathematical model for wet-casting that confirmed the presence of this supersaturated region when macrovoids were observed experimentally. This supersaturated region causes instantaneous demixing.

Matz developed an effective way to directly observe the film formation by phase inversion [35]. In his work, an optical microscope was used to observe the phase inversion process. The observation is achieved by clipping a drop of polymer solution between two glass slides and contacting it with a nonsolvent. This method can provide evidence for elucidating the formation of macrovoid [37, 50].

From the above literature review, the already existing macrovoid formation mechanisms are established from various polymer/solvent/non-solvent systems and there is no mechanism universally applicable. In these studies, most macrovoids root just below the dense skin layer and expand across the whole cross-section of the membranes, taking on tubular-like or tear-like. For the special case of PSf/DMF/water system, the macrovoids can be spherical and suspend at the median of the cross-section of the membrane. Such unique occurrence of macrovoids can not be satisfactorily interpreted from the generally accepted mechanisms, thus needs to be comprehended. Herein, we perform a direct observation of the phase separation for PSf polymer solution when DMF and water are imployed as solvent and nonsolvent respectively. Then flat sheet membranes with the same dope formulations and under similar phase separation conditions are prepared by immersion precipitation method. The microstructure formation mechanism, especially the one for

macrovoid, will be proposed according to the optical observation results combined with the SEM images of the flat sheet membranes. Finally, the relationship between the occurrence of macrovoid and mechanical property of the membranes will be explored.

2. Experimental

2.1. Materials

Commercial polysulfone (Udel ® P-3500, Mn～22kDa, Solvay.) was involved in the experiments. N,N-dimethylformamide (DMF, Chengdu Kelong Chemical Co., Ltd. purity>99.5%, Analytical reagent) and distilled water were used as solvent and non-solvent respectively. Before use, DMF was treated by activated 4A-molecular sieve (Chengdu Kelong Chemical Co., Ltd.) for at least 24 hours to fully remove the water impurity therein.

2.2. Membrane formation

The flat sheet membranes were prepared by immersion precipitation. PSf was pretreated in a vacuum oven at 100 °C for 12 hours prior to use. Polymer dope solutions of different constitution were obtained by adding PSf beads to DMF while stirring rapidly at room temperature in a tightly sealed glass conical flask. Ater 24 hours' stir, the PSf solutions were left to stay still for another 24 hours to remove the air bubbles. A casting knife with a fixed height of 300 μm was used to hand cast the polymer solutions on a glass plate. The casted films were then immediately immersed in the coagulation bath at 25 °C. During the casting process, relative humidity of the surrounding air was about 60%. The nascent membranes were kept in the bath for 30 min to let the films be fully precipitated and then transferred to another distilled water bath to remove the residual solvent.

After that, membranes were air dried at room temperature before further characterizations.

2.3. Characterization

2.3.1. Visualization of phase separation

The phase separation process was directly observed using an optical microscope (Jiangnan XP-201, China) with with 4× objective lens and recorded using a digital camera (JVC TK-C721EC, Japan) at 10× magnification. Sample preparation was performed as described by Matz [35]. A drop (～20 μl) of the dope solution was placed between a glass slide and cover slip. Then the edge of the cover slip was touched with a drop of non-solvent. The non-solvent quickly infiltrate into the clearance to contact the rim of the spread thin polymer solution. Pictures of the phase separated film were taken every 30 seconds and analyzed by Image-Pro-Plus software for further theoretical calculation.

2.3.2. Membrane morphology

The obtained hand casted membranes were freezing fractured by liquid nitrogen to prepare the membrane cross-sections. Samples were then dried overnight at room temperature before mounted on the SEM sample holders and coated with gold to prevent charging. A Hitachi S-4800 field emission scanning electron microscope (FE-SEM) was used to take images of membrane cross-sections and top surfaces.

2.3.3. Porosity measurement

The porosity was measured by calculating the water occupied volume ratio of the membrane

when maintained in distilled water. It is operated by the following steps: the wet membranes were cut into rectangular pieces and weighed after mopping the superficial water with filter paper. Then they were dried in an oven at 60 °C for 24 hours and further dried at 80 °C for another 24 hours before weighed again. Finally, the porosity of membrane can be obtained by using the following equation [51]:

$$P(\%)=\frac{(W_w - W_d)}{\rho_w \times A \times h}\times 1000 \quad (1)$$

where $\boldsymbol{P}$ is porosity of membrane, $\mathbf{W_w}$ is the weight of wet sample (g), $\mathbf{W_d}$ is the weight of dried sample (g), $\boldsymbol{\rho_w}$ is the density of pure water (g/cm^3), $\boldsymbol{A}$ is the area of the tailored wet sample (cm^2), and $\mathbf{h}$ is the thickness of the wet sample (mm). Each measurement was repeated for 3 times and the calculated average value of $\boldsymbol{P}$ was taken as the testing result.

2.3.4. Compression test

Resistance to compaction of the membranes was evaluated by applying compression testing on a universal testing machine CMT6104 from MTS. To ensure proper compression loading conditions, accurate specimen preparation, a perfect fit between the specimen and the compression plates, as well as correct alignment of the specimen and load introduction devices are crucial [52]. Thus, we explored the testing conditions and established the testing method, which is under adequate conditions for proper characterization of the resistance to compaction property. We determined that all the tests were carried out under the same conditions: (i) samples were tailored to form 1.5×1.5 cm square-like films and mounted between two compression plates; (ii) the tests were carried out at 25°C by applying strain rate of 0.5 mm/min; (iii) the upper limit of the load employed was fixed at 5 kN. Each test was repeated 3 times to ensure its reproducibility.

3. Results and discussion

3.1. Observation of phase separation from PSf/DMF/water system

3.1.1. Variable PSf concentration

Polymer solutions with 12 wt%, 15 wt%, 18 wt%, 21 wt%, and 24 wt% PSf were prepared using DMF as the solvent. Though direct observation technique on optical microscope suffers from a few shortcomings, basically the difficulty in controlling the sample geometry, this technique does, however, allow for the real time measurement of macrovoid formation and uses only a small amount of material, so it can be still used to rapidly evaluate the phase separation process from normal polymer/solvent/non-solvent systems. The phase separation process was observed on the optical microscope at 25 °C with distilled water as the non-solvent. As soon as the non-solvent penetrated into the polymer solution, optical micrographs were taken for every 30 s. Cloud point data for the PSf/DMF/water system calculated by Barth et al. [18] shows that only a small amount of water (1–2 wt%) is required to induce phase separation. Guillen et al. [23] found that the phase separation began to occur before the introduction of non-solvent because of the high surrounding relative humidity (40%-50%). In light of this, to prevent the beginning of phase separation of the polymer solution rim before it is contacted with non-solvent, we placed about 20 μl polymer solution, which is more than usual (～10 μl), onto the glass slide and rapidly put on the cover slip. The introduction of non-solvent must be fast enough as well. Fig.1 shows the time sequence images of the phase separation process of polymer solution with different PSf concentration after dropping the non-solvent. The fringe-like cavities, at the edge of already phase separated film, can be found in all these pictures. This implies that phase separation of the

polymer solution rim did not happen before the introduction of distilled water, even though the laboratory RH reached 60% high. When non-solvent is introduced, an additional pressure can arise between the two glass slides due to the wetting of water to the glass with strong hydrophilicity. Under such pressure, formation of these fringe-like cavities can be related to the viscous fingering phenomenon which is evolved from the flow instability resulting from a less viscous fluid displacing a more viscous fluid. This phenomenon is kind of far from equilibrium pattern formation [53]. With time going on, macrovoid free structure was developed underneath the layer containing fringe-like cavities, and void formation by coalesce of phase separated polymer rich phase was observed (PSf concentration ≥ 18 wt%).

The penetration rate can be evaluated with the method recommended by Strathmann et al. [37]:

$$d=2(D_e t)^{1/2} \quad (2)$$

where **d** is the penetration distance, $\mathbf{D_e}$ is the apparent diffusion coefficient of a nonsolvent and **t** is the time. The moving distance (**d**) of the precipitation front at different times can be measured by an image processing software. Then, penetration distance of non-solvent can be plotted as function of square root of time (Fig. 2(a)). The $\mathbf{D_e}$ can be calculated from Eq. (2) using the slope obtained from linear regression method (Fig. 2(b)). The derived $\mathbf{D_e}$s are substantially lower than the theoretically mutual diffusion coefficient of DMF and water ($1.25\times10^{-5}cm^2/s$) when PSf concentration is higher than 18 wt%. The results indicate that the diffusion rate of the non-solvent into the polymer solution can be reduced with elevated PSf concentration. It is believed that the phase separation process is controlled by the trade-off between thermodynamic enhancement and kinetic hindrance [20]. When PSf concentration is high enough, the resultant high viscosity of the polymer solution can play an important role as kinetic hindrance in determining the diffusion rate

of non-solvent into the polymer solution, thus influence the phase separation process. Considering the little change in thermodynamic instability of polymer dope solution when increasing the PSf concentration, the strange phenomenon that $\mathbf{D_e}$ is not sensitive to PSf concentration above 15 wt% might come from another kinetic factor. As the polymer concentration increases, the nascent phase separated bi-continuous structure will be more crowded, resulting in the increased interfacial energy. Consequently, the phase separated polymer rich phase tends to coalese more easily. The contraction force of the network, owing to the increased coalescence trend of the phase separated polymer rich phase, will increase, leading to accelerated convection flow of phase separated polymer lean phase into the dope solution, diffusion rate of water is speeded up. Hence, when increasing PSf concentration, the trade-off effect, between increased kinetic hindrance of water diffusion and increased convective water influx into dope solution, determines the rate of phase separation. This effect leads to the insensitivity of the calculated $\mathbf{D_e}$ when PSf concentration is above 15 wt%.

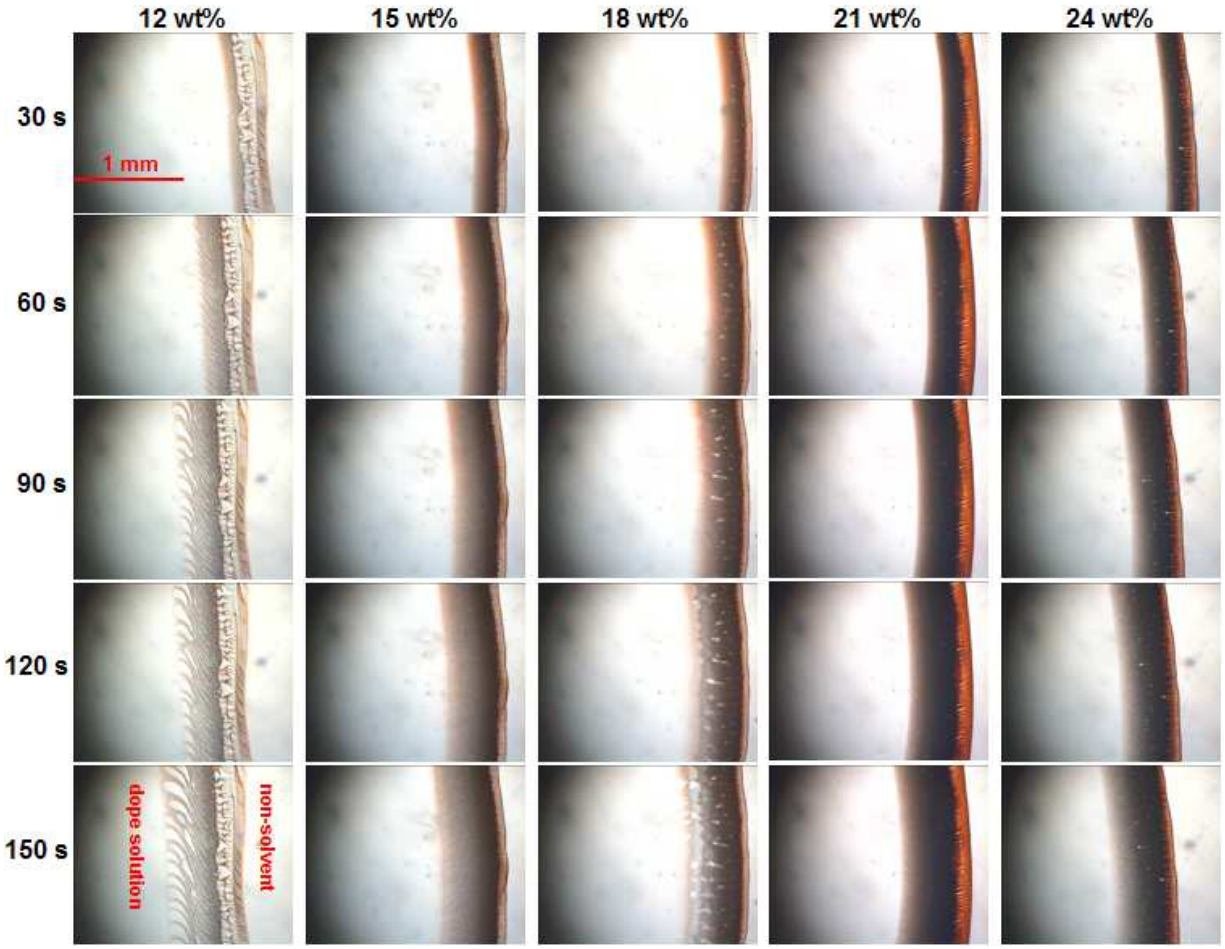

Fig. 1. Optical micrographs (magnification: 40×) for the nonsolvent (distilled water) penetration with time into polymer solution (DMF as solvent) containing variable PSf concentration (wt%). The vertical and horizontal numbers represent the penetration times and PSf concentrations respectively.

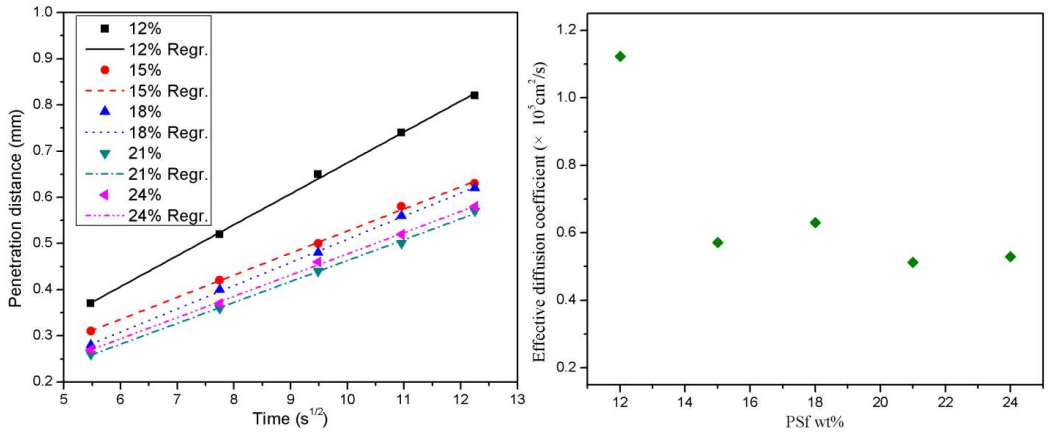

(a) (b)

Fig. 2. Pictures showing penetration rates of pure water into polymer solutions with different PSf concentrations: (a) penetration distance of non-solvent vs. square root of time; (b) effective diffusion coefficient vs. PSf concentration in polymer solution.

3.1.2. Variable coagulation bath constitution

The phase separation optical micrographs were also obtained as shown in Fig.3 when non-solvent with different DMF concentrations (10 wt%, 30 wt%, 50 wt%, 70 wt%, and 90 wt%) was used as the coagulation bath for fixed polymer solution (18 wt% PSf-82 wt% DMF). The penetration rate of non-solvent with different DMF concentration into polymer solution is described in Fig. 4(a) and Fig. 4(b). The results reveal that the diffusion rate of the water into polymer solution will not be greatly reduced until the concentration of DMF in the coagulation bath exceeds 70 wt%. As is suggested above, when thermodynamic condition of the polymer solution keeps the same (18 wt% PSf), the phase separation process is determined by kinetic factors. The precipitation of PSf during phase separation process can be treated as a layer by layer consolidation event [54]. Diffusion of non-solvent into the layer where phase separation sets in will be influenced by the already consolidated PSf layer above. With increasing the DMF concentration in the coagulation bath, coarsening of the phase separated polymer lean phase or coalescence of the phase separated polymer rich phase will have enough time to take place, leading to the formation of a more porous structure in the consolidated layer. Thus the trade-off, between the lowered chemical potential of water in the coagulation bath and the elevated permeability of the already consolidated more porous layer, is the main kinetic factor that will determine the rate of phase separation. When the concentration of DMF is high enough (≥70 wt%), lowering of chemical potential of water overwhelms the formation of more porous structure, the rate of phase separation will be reduced.

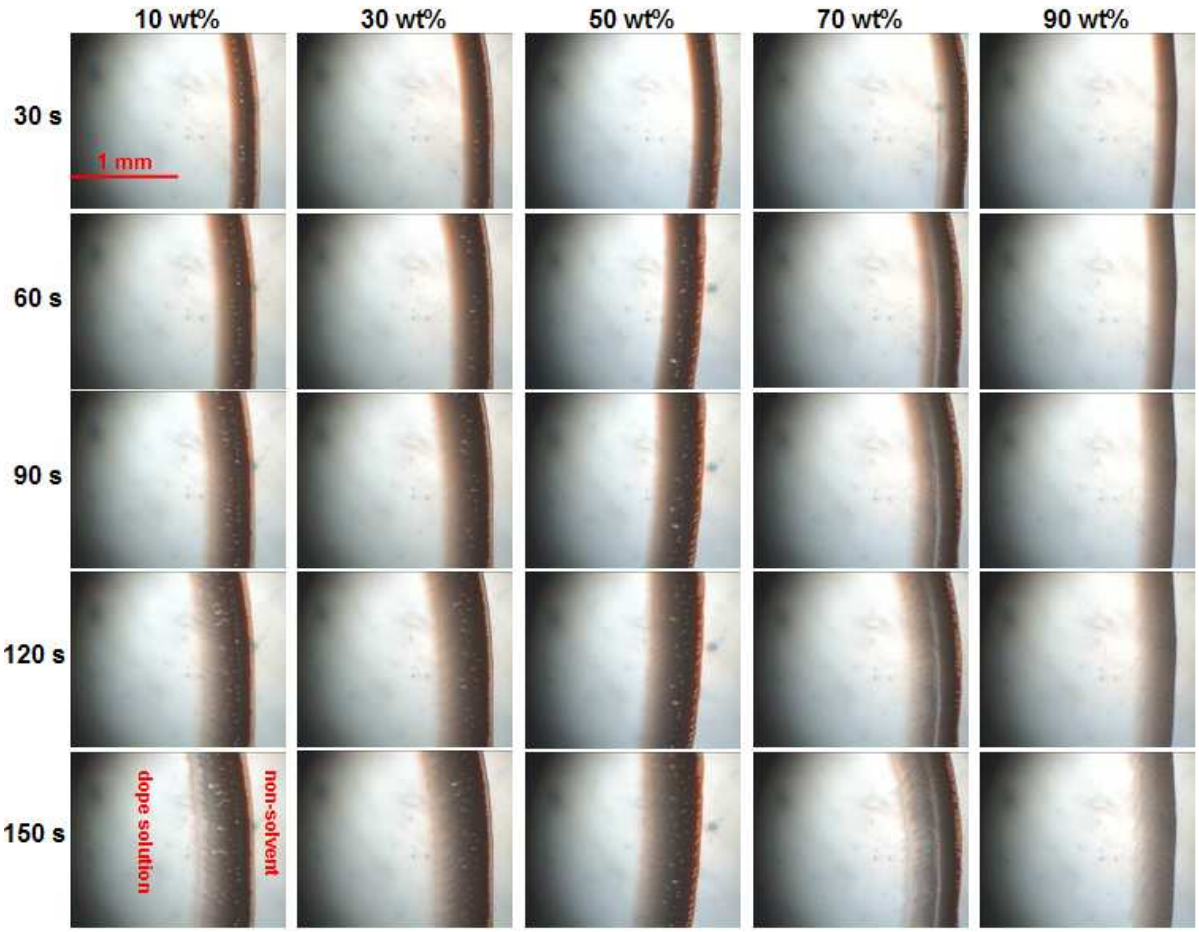

Fig. 3. Optical micrographs (magnification: 40×) for the nonsolvent (different mass fraction of DMF) penetration with time into fixed polymer solution (18 wt% PSf-82 wt% DMF). The vertical and horizontal numbers represent the penetration times and DMF concentrations respectively.

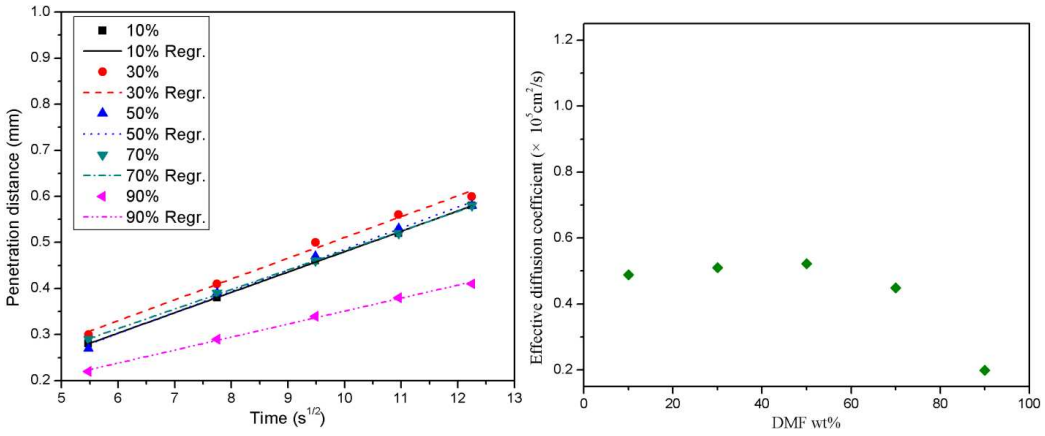

Fig. 4. Pictures showing penetration rates of non-solvent with different DMF concentrations into fixed polymer solution (18 wt% PSf-82 wt% DMF): (a) penetration distance of non-solvent vs. square root of time; (b) effective diffusion coefficient vs. DMF concentration in gelation bath.

3.1.3. Macrovoid formation and proposed mechanism

An interesting formation process of macrovoid was observed a few minutes after the introduction of non-solvent. As the penetration continued, there appeared a transparent band (180s after introduction of water to 15 wt% PSf polymer solution and 240s after introduction of 50 wt% and 90 wt% DMF coagulation bath to 18 wt% PSf polymer solution in Fig. 5) at the front of the phase separating interface. When PSf concentration is high enough (≥21 wt%), existence of this band was vague. It is easy to understand that the transparent band is caused by the difference in local refractive index of polymer solution with different PSf concentration. Tens of seconds later, macrovoid initiation was found at the front of the phase separating interface. The growth direction of macrovoids is latitudinal at the beginning and then longitudinal, until they fill the transparent band to form a lattice-like structure. The edges of the adjacent macrovoids can get stuck, leading to the merging phenomenon of the macrovoids. Polymer beads were also formed within the macrovoids during this process. This kind of beads are conventionally formed by a secondary phase inversion in the polymer lean phase where polymer concentration of the dope solution is located under that of the critical point in phase diagram [55]. If the polymer concentration of transparent band is low enough, initiation of macrovoids can be caused by the mechanism of nucleation and growth of polymer rich phase. Actually, there might exist such polymer lean layer whose PSf concentration can be lower than that of the critical point. Basically, this layer can be expected to be formed by diffusion of solvent into the dope solution. As the diffusion rate of solvent from the dope solution can not be fast enough to cause the formation of this polymer lean layer, diffusion of solvent into this layer might come from elsewhere. With further results from the

SEM picture of the immersion membrane (Fig. 6 (a)) showing that the microstructure beneath the dense skin layer takes on bi-continuous which is said to be formed by the spinodal decomposition mechanism [14], we can expect that bi-continuous structure will also be developed during optical observation experiments (Fig. 6 (b)). As phase separation proceeds, the contraction of the spinodal decomposition formed network of polymer rich phase will cause inflow of the already phase separated polymer lean phase to the polymer dope solution. Then, diffusion of solvent from the continuous polymer lean phase into the dope solution can be easily achieved, leading to the formation of such polymer lean layer. Lee et al. [44] developed a detailed mathematical model in which they allowed for convection that arises owing to the densification that occurs when non-solvent penetrates the casting solution. This non-buoyancy density-driven convection accelerates the influx of non-solvent by orders of magnitude early in the wet-casting process. When this density-driven convection is included, the model predicts the presence of a supersaturated region that promotes macrovoid growth. Based on these findings, the formation mechanism of macrovoid from PSf/DMF/water system can be comprehended as illustrated in Fig. 7. Density-driven convection of bi-continuous region can lead to the development of a polymer lean layer, further influx of water drives the formation of supersaturated regions, trigger of phase separation by the mechanism of nucleation and growth of polymer rich phase in these regions will initiate the formation of macrovoids in the transparent band, macrovoids will further grow into tear-like structure because of the lateral contraction of polymer rich phase formed network and consecutive inflow of phase separated polymer lean phase. This model is quite unconventional because macrovoid formation is usually believed to be initiated from phase separated polymer lean phase and macrovoid growth is related to the diffusion of solvent expelled from the

surrounding polymer solution [34]. Therefore, we will validate our proposed mechanism practically in the following sections.

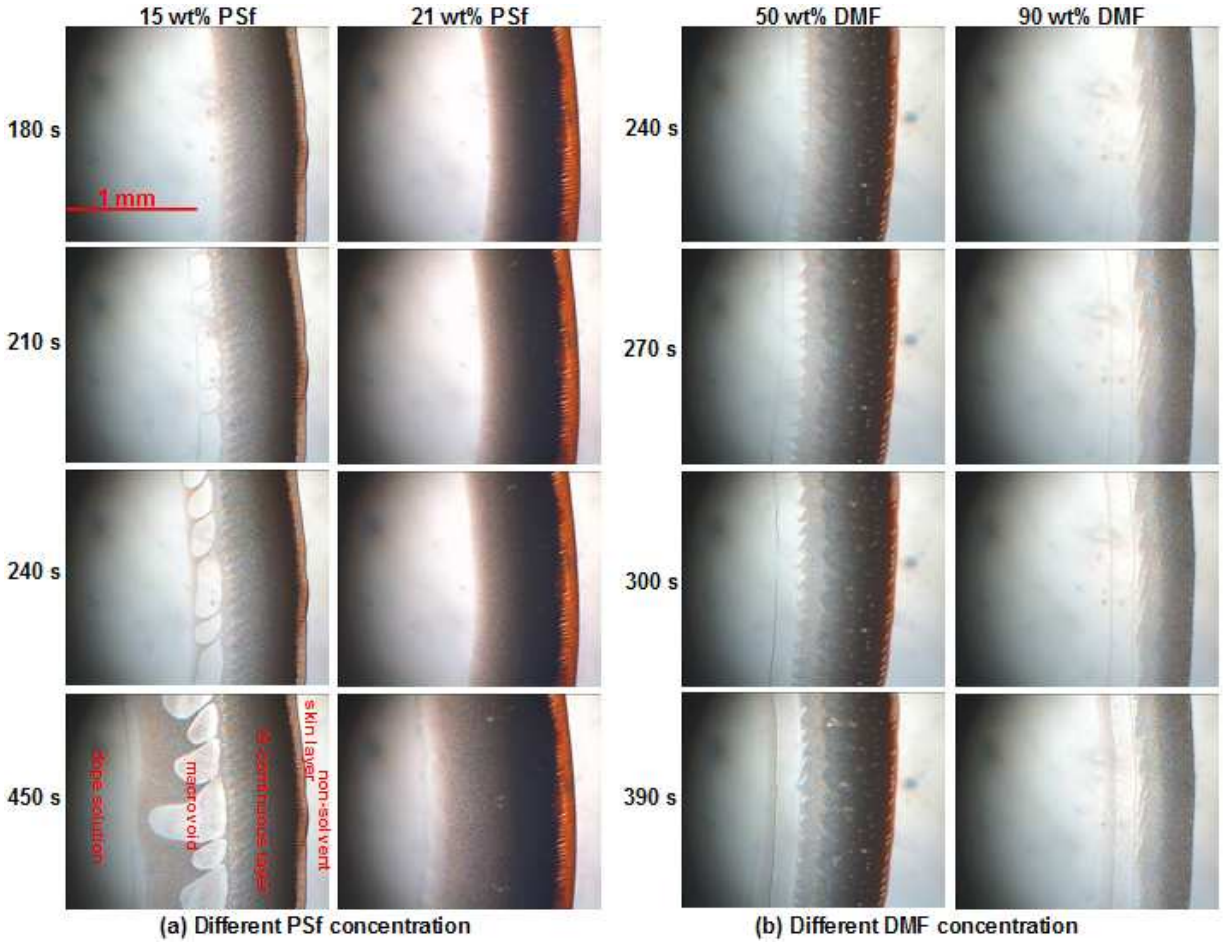

Fig. 5. Occurrence of macrovoid formation in (a) phase separation processes from water (pure water coagulation bath) diffusion into polymer solutions with different PSf concentration and (b) phase separation processes from coagulation bathes with different DMF concentration (PSf concentration fixed at 18 wt%).

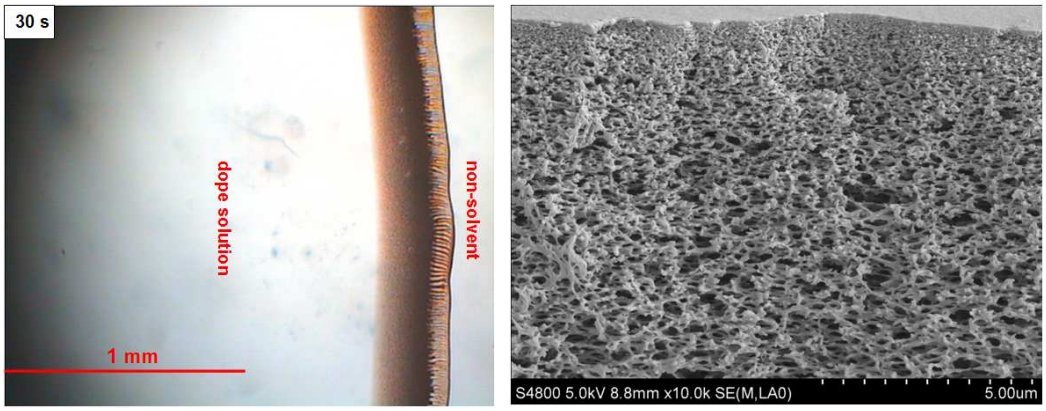

(a) (b)

Fig. 6. Comparison of bi-continuous region of optical micrograph and the SEM picture: (a) optical micrograph at 30 s for pure water penetrating into 15 wt% PSf dope solution; (b) SEM picture of membrane prepared with 15 wt% PSf dope solution when pure water was used as gelation bath.

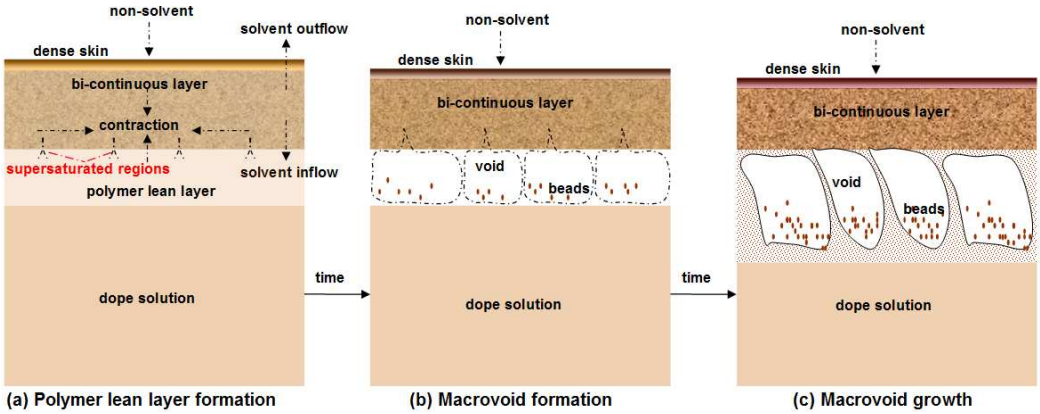

Fig. 7. A diagrammatic sketch of the macrovoid formation mechanism from PSf/DMF/water.

3.2. Macrovoid occurrence in phase inversion membranes

In order to relate the optical observation results to the formation of immersion precipitated membranes, and verify the feasibility of the proposed macrovoid formation mechanism in phase inversion membranes from PSf/DMF/water system. We prepared PSf membranes under the conditions similar to that for direct visualization of phase separation.

3.2.1. Macrovoid formation damped by polymer concentration

The SEM cross-section and top surface images of membranes prepared from polymer dope solutions with different PSf concentration are presented in Fig. 8. These pictures reveal that the formation of macrovoid and porous top surface is obviously damped with increasing the PSf concentration. Bi-continuous structure can be found beneath the dense skin layer for all samples. It is interesting that the shape of macrovoid evolves from finger-like to sphere-like and all the macrovoids emerge under a certain distance from the top surface. For PSf concentration reaches

15 wt%, the macrovoids even suspend at the middle of the cross-section.

The pinhole-like pores on top surface has been ascribed to irregular packing of kinked polymer chains and incomplete coalescence of polymer molecules in skin layer [56]. Their size can be determined by the order of events during phase separation [26-28]. Top surface with smaller pores can result from the faster gelation process of the concentrated polymer phase than that of the coarsening and coalescence of phase separated polymer rich phase. On the contrary, larger pores are formed when the coarsening and coalescence effect overwhelms the gelation process. Gelation of more concentrated top surface will be expected to gradually dominate the coarsening and coalescence phenomenon with increasing PSf concentration in the polymer dope solution, leading to the formation of smaller pores on top surface.

For the formation of bi-continuous structure underneath the dense skin layer, spinodal decomposition mechanism is involved [14]. The theoretically calculated phase diagram of PSf/DMF/water system by Barth et al. [18] depicts a narrow homogeneous region and large spinodal decomposition region, indicating that the polymer solution can be able to rapidly cross the meta-stable region without phase separation and reach the unstable region to go through spinodal decomposition [31]. Kuo et al. [32] observed that during vapor induced phase separation (VIPS), the nascent bi-continuous structure can be formed by spinodal decomposition and coarsened to cellular pores when solvent of low volatility was adopted. As the surrounding RH is high (～60%) and only a small amount of water (1–2 wt%) can induce phase separation of PSf/DMF/water system [31], even a short time interval between the casting and immersion step can be enough to let the casting film imbibe water to go through VIPS, hence spinodal decomposition is favored and bi-continuous structure can be retained by the coagulation bath.

Tiraferri et al. [6] prepared PSf membrane from a 9 wt% PSf-91% DMF dope solution, uniform finger-like macrovoids spanning the layer thickness were obtained. This is in accordance with our finding where the similar finger-like macrovoids were found when PSf concentration was reduced to 12 wt%. They claimed that for the 9 wt% PSf solution, slow demixing conditions cannot be sustained because of the low solution viscosity, thereby resulting in the formation of macrovoids in the sublayer [34]. But they did not explain why these macrovoids rooted at a certain distance away from the top surface. Smolders et al. [34] explained this phenomenon by suggesting that macrovoids are initiated by freshly formed nuclei of the diluted phase when a change in precipitation conditions from instantaneous to delayed onset of demixing occurs at a certain distance from the film interface. But generally this change of precipitation conditions occurs close to the interface, leaving a relatlvely thin skin (~0.2 μm typically) of a different structure. Macrovoids derived by this mechanism can be rooted at a certain distance away from but very closed to the top surface of the membrane. This structure is very different from that observed in our PSf/DMF/water system where the macrovoids are rooted at over 10 μm away from the top surface. Thus, the even suspended macrovoids, at the middle of the cross-section of the membranes prepared with 15 wt% and 18 wt% PSf concentration, might result from some other mechanism.

With the former proposed macrovoid formation mechanism, this unique occurrence of macrovoid can be well interpreted. After the spinodal decomposition induced formation of bi-continuous region, a polymer lean layer can be developed beyond the non-solvent intrusion frontier. This layer can be rooted far away from the membrane surface. When the PSf concentration of this layer is lower than the critical point, further diffusion of water into it can induce phase separation. Rapid growth of continuous polymer lean phase leads to the formation of

horizontal macrovoids. These macrovoids might be further squeezed to be tear-like or finger-like with slow gelation accompanied local contraction.

The PSf concentration at the critical point is about 11 wt% from theoretical calculation [18]. When PSf in dope solution reaches 21 wt% high, the constitution of the polymer lean layer can hardly be located below the critical point because of the less formed polymer lean phase by spinodal decomposition and the low diffusion rate of solvent into this boundary layer. Consequently, macrovoid formation is damped.

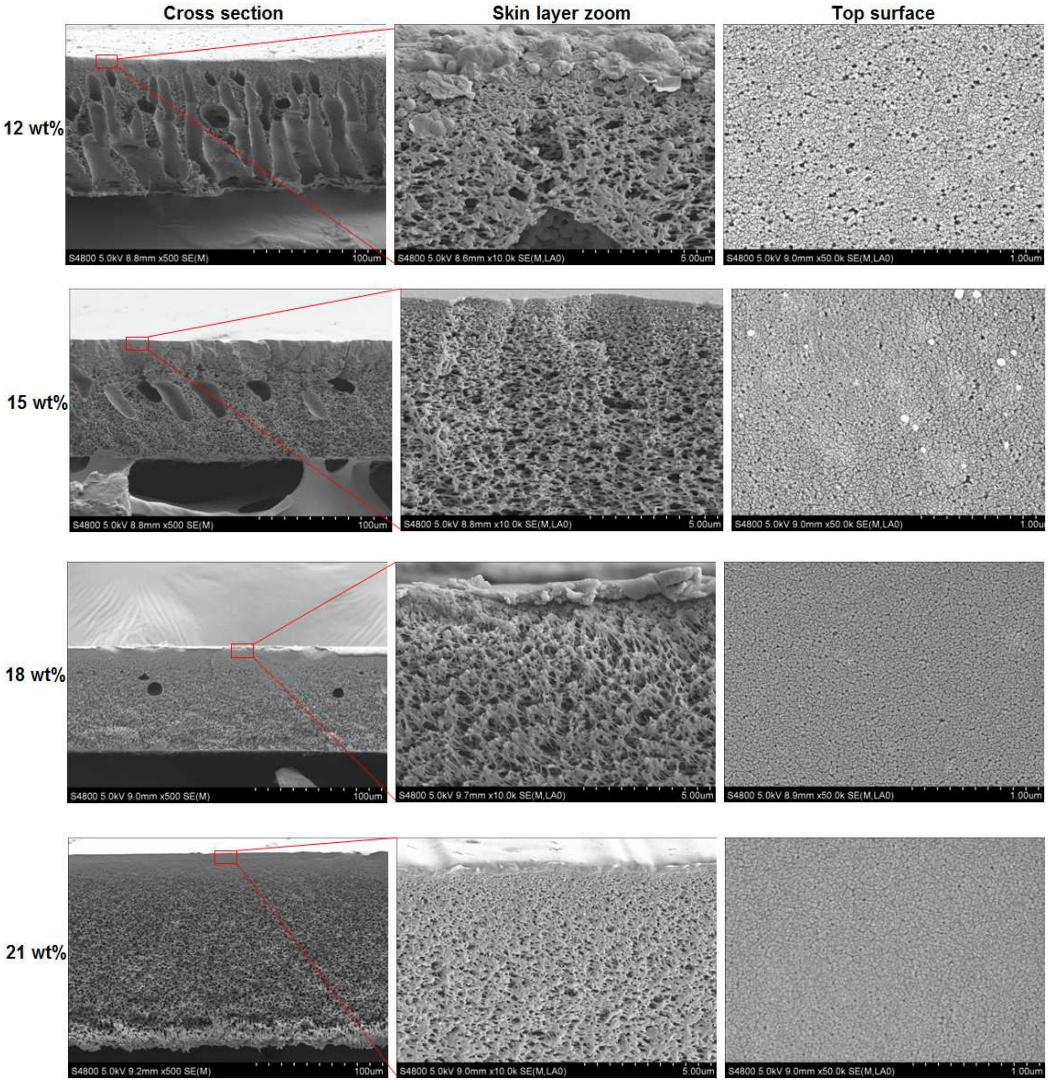

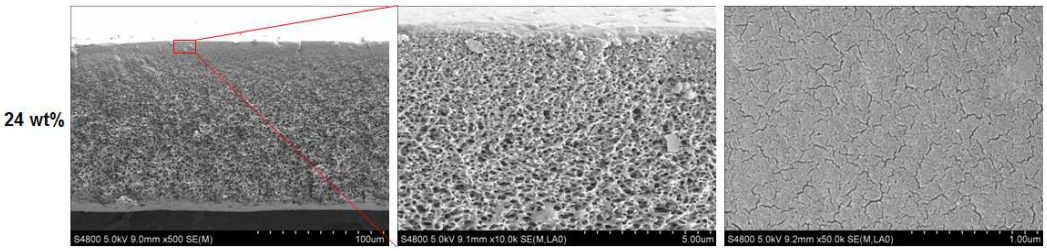

Fig. 8. SEM cross-section and top surface images of membranes prepared from polymer dope solutions with different PSf concentration. Distilled water was used as coagulation bath.

3.2.2. Unique macrovoid occurrence resulting from different coagulation bath constitutionsin

Fig. 9 exhibits the SEM cross-section and top surface images of membranes which were prepared by immersion precipitating fixed 18 wt% PSf dope solutions in coagulation bathes with varied DMF concentration. Larger pores on the top surface were also found when more DMF was added to the coagulation bath, this is due to the increased timescale for the coarsening and coalescence phenomenon. Macrovoids were not damped by adding the DMF solvent into coagulation bath and rather, their appearance moved close to the top side of the membrane when DMF in coagulation bath exceeded 70 wt%. As revealed in the zoomed pictures of the skin layer (70 wt% and 90 wt% DMF in coagulation bath), they were found to be rooted in the bi-continuous region.

Usually, the rate of phase separation can be slowed down by adding solvent in coagulation bath to decrease the exchange rate between solvent and non-solvent. If the solvent concentration in coagulation bath is high enough (generally lower than 70 wt%), instantaneous demixing will be inhibited, delayed demixing is achieved. Then initiation of macrovoids by a change in precipitation conditions from instantaneous to delayed onset of demixing can never take place, macrovoids are damped. From the previous study, it is observed that the rate of phase separation can be greatly reduced when the DMF concentration exceeded 70 wt%. Under this condition, we

can conclude that delayed demixing has already been achieved. But macrovoids were still observed in this case, even when the DMF concentration was elevated to as high as 90 wt%. Thus, the most classical mechanism of macrovoid formation hypothesized by Smolders et al. [34] is failed here to explain why damping of macrovoids will not be achieved by adding solvent in coagulation bath. Yet, with the mechanism proposed in the light of direct observation of phase separation from PSf/DMF/water system, such unique occurrence of macrovoids can be quite reasonable. Increasing DMF in coagulation bath will lower the chemical potential of water diffusion into polymer dope solution, leading to the slow phase separation process especially for DMF exceeds 70 wt%. With the decreased rate of PSf consolidation, the reduced DMF outflow, the smaller contraction force of the network constructed by bi-continuous polymer rich phase, as well as the less outflow of phase separated polymer lean phase, diffusion of DMF into the dope solution will draw the polymer lean layer with constitution below the critical point near the top surface. Then, with further diffusion of water, phase separation takes place, macrovoids settle in. The occurrence of finger like pores at the skin layer of the membrane at 90 wt% DMF concentration might be also related to the obviously lowered phase separation rate. Under such condition, the initiated macrovoids have enough time to grow, and with the contraction force developed by the slow gelation of the phase separated polymer rich phase, they can be squeezed to form the finger like pores. As for the remarkable phenomenon that these macrovoids are rooted in the bi-continuous region, Prakash et al. [57] found the similar exclusive location pattern from a quaternary system of PSf/DMAC/THF/ethanol. They related this feature to a sequence of events during phase separation process, including: (i) a roughly in-plane solidification front of the polymer rich phase; (ii) elastic tensile stress developed in the solidified polymer phase; (iii) the arising uniaxial elastic

tensile stress with time; (iv) break of the connecting necks of the matrix network; (v) growth and formation of macrovoid induced by the pressure build-up in the polymer lean liquid. For phase separation from PSf/DMF/water ternary system, the occurrence of macrovoids rooted in the bi-continuous region is a strong evidence for our previously proposed mechanism of macrovoid formation. The contraction of bi-continuous polymer rich phase induced inflow of phase separated polymer lean phase and successive diffusion of non-solvent can actually result in this unique feature. It should be pointed out that the proposed mechanism for macrovoid formation seems to be not sample specific. For the polymer/solvent/non-solvent systems, which lead to the formation of the similar cross-section morphology of the membranes as that developed from PSF/DMF/water system, this mechanism might be also applicable. For example, phase separation process of the immersion precipitated membranes from the work of Prakash et al. [57] and Kosma et al. [46] could be explained with this mechanism.

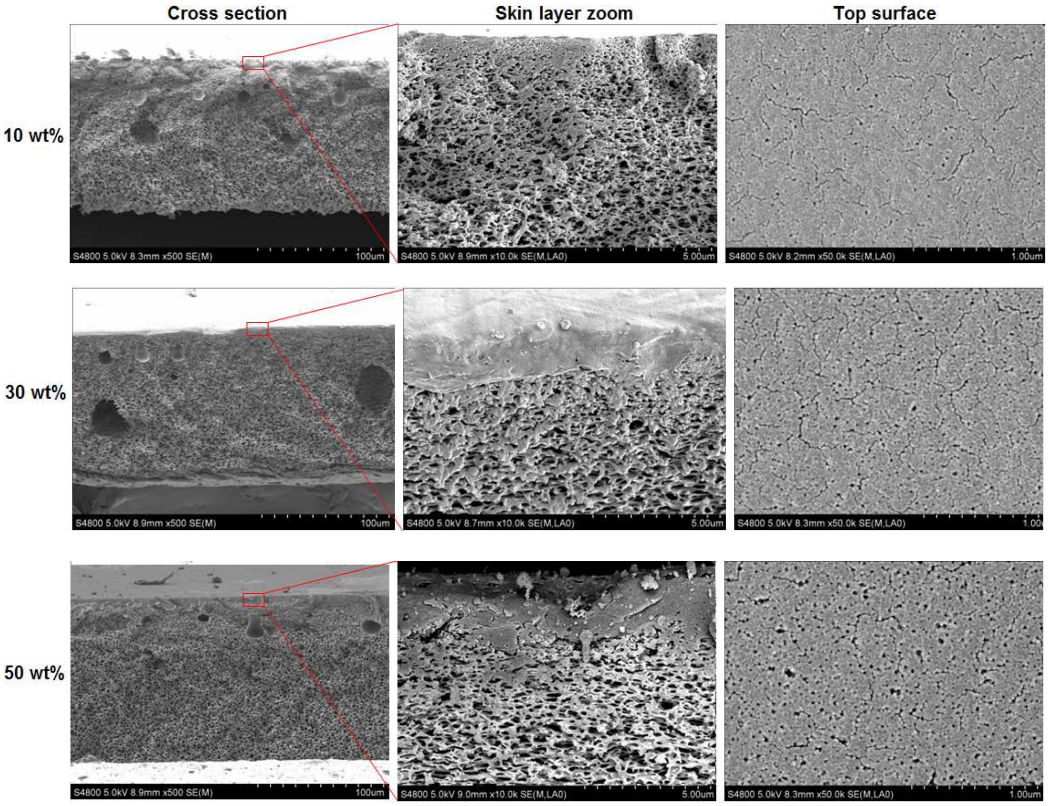

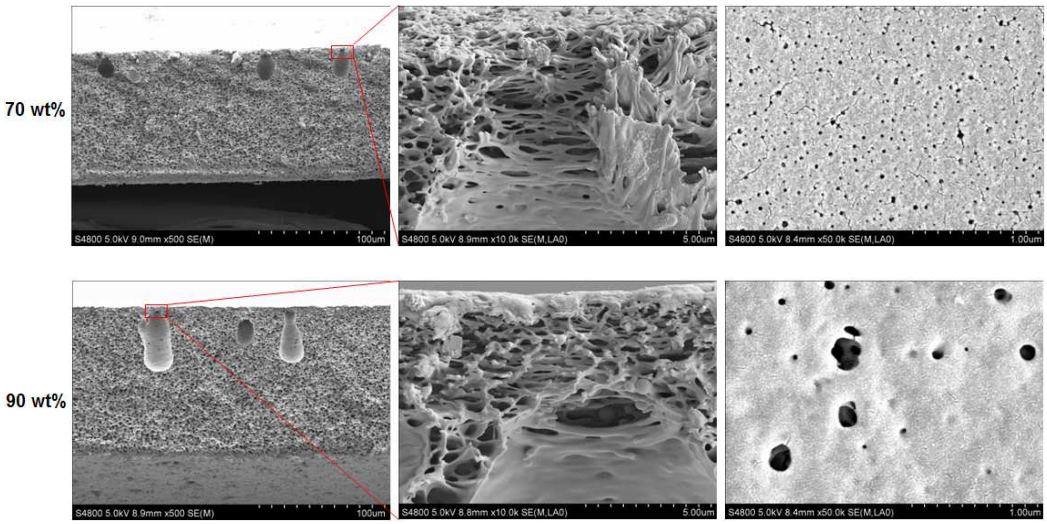

Fig. 9. SEM cross-section and top surface images of membranes prepared from polymer dope solutions with fixed 18 wt% PSf concentration. The immersion coagulation bathes consist of different DMF concentration.

3.3. Influence of macrovoid on mechanical support application

The mechanical properties of the membranes can be detected by either tensile [58] or compaction test [59]. PSf membranes prepared by immersion precipitation are attractive in application for support layer of thin film composite (TFC) membrane. For seawater reverse osmosis (SWRO) desalination, the mechanical property of the support layer, especially the resistance to high hydrostatic pressure, is crucial because the employed pressure during SWRO process can achieve as high as 60 bar. Though PSf possesses distinctive mechanical property, the existence of macrovoids within the PSf-support layer might reduce its resistance to the external stress greatly. Herein, we developed a new method to assess this mechanical property of the membranes by applying compression testing on a universal testing machine. Membranes prepared from dope solutions with variable PSf concentration showed large changes in occurrence of macrovoid, thus were discussed here to elaborate the influence of macrovoid structure on compaction resistance property.

The strain of the membranes were too difficult to be detected because of their tiny thickness and the relatively great strain of the metallic parts of the machine during the tests. We recorded the stress-displacement curves with that of the testing machine (no sample was loaded) as contrast to reveal the response of membranes under mechanical compression. Yield strength was determined using the offset method, by tracing a line parallel to the slope of the elastic part of the curve at a 0.005 mm displacement. The intersection of this line and the stress–displacement curve defines the offset yield strength. The stress–displacement curves of the membranes are presented in Fig. 10(a). A typical fracture behavior with a yield stress and following yield point jog is observed during the test. It is obvious from the result that membrane prepared with higher PSf concentration in dope solution possesses higher yield stress. The obtained offset yield stress as well as the porosity of the membranes were furtherly plotted as function of PSf concentration which is presented in Fig. 10(b). They both show well linear relationship with PSf wt%. The offset yield stress exceeds 60 bar when PSf concentration reaches 18 wt%, implying that membrane prepared from dope solution with PSf concentration larger than 18 wt% can withstand the pressure in SWRO application. Combined with the SEM results, we can conclude that, when PSf concentration is below 18 wt%, the porosity decreases with increasing PSf concentration due to the decreased size and number of macrovoid. While the decreasement of porosity with increasing PSf concentration is owing to the increased consolidatable constitution of polymer in the dope solution if the PSf concentration is above 18 wt%. Offset yield stress increases greatly with reduced porosity due to damped macrovoid formation in the cross-section of membranes. Hence, it can be concluded that the occurrence of macrovoid will cause negative effect on mechanical property of the membranes.

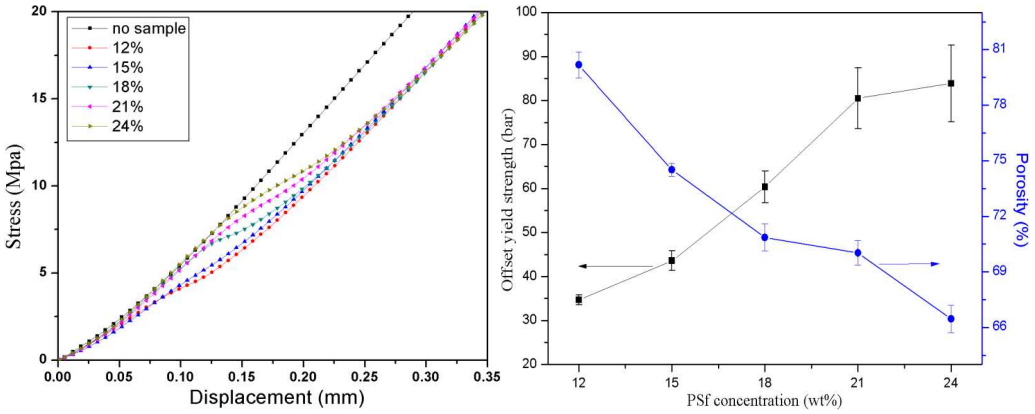

(a) (b)

Fig. 10. (a) Stress-displacement curves and (b) 0.005 mm displacement offset yield strength and porosity of membranes prepared from polymer dope solutions with different PSf concentration. Distilled water was used as coagulation bath.

4. Conclusions

Phase inversion process from a ternary system of PSf/DMF/water was visualized with an optical microscope. PSf concentration in polymer solution and DMF in coagulation bath, taken as the thermodynamic and kinetic factors respectively that influence the phase separation process, were studied in this paper. Results showed that both factors could alter the phase separation process by a trade-off effect between thermodynamic enhancement and kinetic hindrance. Apparent diffusion coefficient of water into PSf solution, which was calculated from a kinetic model, indicated that the rate of phase separation due to intrusion of water could be reduced by increasing PSf concentration in polymer solution or increasing DMF concentration in coagulation bath. Unique occurrence of macrovoid was directly observed at the later stage of phase separation, combined with the SEM cross-section images of immersion precipitated membranes, we came up with a mechanism to elucidate the formation of macrovoid from PSf/DMF/water system. This

mechanism basically involves the development of a transition polymer lean layer whose constitution may determine the formation of macrovoid or not. The damping of macrovoid by elevated PSf concentration in dope solution, the failure in eliminating macrovoid by introduction of DMF solvent in coagulation bath, as well as the unique occurrence and location of macrovoid at the cross-section of immersion precipitated membranes can be well interpreted by applying this mechanism. Finally, a novel method was employed to test the mechanical resistance to compaction of the membranes. The occurrence of macrovoid is then correlated with mechanical performance successfully. Results showed that they had fine relevance. It is concluded that membrane is mechanically more sustainable with damping of macrovoid.

Acknowledgement

The authors would like to sincerely thank Vontron Technology Co.,Ltd. for the financial support of this study.

References

1. S. Loeb and S. Sourirajan, *Sea water demineralization by means of an osmotic membrane*, ACS Publications, 1962.
2. M. Mulder, *Basic Principles of Membrane Technology Second Edition*, Kluwer Academic Pub, 1996.
3. G. R. Guillen, Y. Pan, M. Li and E. M. Hoek, *Ind. Eng. Chem. Res.*, 2011, 50, 3798-3817.
4. M. Jeon, S. Yoo and C. Kim, *J. Appl. Polym. Sci.*, 2008, 107, 1194-1200.
5. S. Tan, L. Li, Z. Zhang and Z. Wang, *Chem. Eng. J.*, 2010, 157, 304-310.

6. A. Tiraferri, N. Y. Yip, W. A. Phillip, J. D. Schiffman and M. Elimelech, *J. Membr. Sci.*, 2011, 367, 340-352.

7. J. T. Arena, B. McCloskey, B. D. Freeman and J. R. McCutcheon, *J. Membr. Sci.*, 2011, 375, 55-62.

8. N. Widjojo, T.-S. Chung, M. Weber, C. Maletzko and V. Warzelhan, *J. Membr. Sci.*, 2011, 383, 214-223.

9. G. Han, S. Zhang, X. Li, N. Widjojo and T.-S. Chung, *Chem. Eng. Sci.*, 2012, 80, 219-231.

10. A. K. Ghosh and E. Hoek, *J. Membr. Sci.*, 2009, 336, 140-148.

11. P. S. Singh, S. Joshi, J. Trivedi, C. Devmurari, A. P. Rao and P. Ghosh, *J. Membr. Sci.*, 2006, 278, 19-25.

12. H. I. Kim and S. S. Kim, *J. Membr. Sci.*, 2006, 286, 193-201.

13. M. G. Buonomenna, *RSC Adv.*, 2013, 3, 5694-5740.

14. M. Beerlage and C. Smolders, *Polyimide ultrafiltration membranes for non-aqueous systems*, Universitiet Twente, 1994. (Ph.D. dissertation).

15. W. Lau, A. F. Ismail, N. Misdan and M. Kassim, *Desalination.*, 2012, 287, 190-199.

16. G. Z. Ramon, M. C. Wong and E. Hoek, *J. Membr. Sci.*, 2012, 415, 298-305.

17. M.-J. Han and D. Bhattacharyya, *J. Membr. Sci.*, 1995, 98, 191-200.

18. C. Barth, M. Goncalves, A. Pires, J. Roeder and B. Wolf, *J. Membr. Sci.*, 2000, 169, 287-299.

19. J.-J. Qin, F.-S. Wong, Y. Li and Y.-T. Liu, *J. Membr. Sci.*, 2003, 211, 139-147.

20. K.-W. Lee, B.-K. Seo, S.-T. Nam and M.-J. Han, *Desalination.*, 2003, 159, 289-296.

21. S. Madaeni and A. Rahimpour, *Polym. Advan. Technol.*, 2005, 16, 717-724.

22. A. Conesa, T. Gumí and C. Palet, *J. Membr. Sci.*, 2007, 287, 29-40.

23. G. R. Guillen, G. Z. Ramon, H. PirouzKavehpour, R. B. Kaner and E. Hoek, *J. Membr. Sci.*, 2013.

24. A. K. Hołda and I. F. Vankelecom, *J. Membr. Sci.*, 2014, 450, 499-511.

25. S. R. Panda and S. De, *J. Polym. Res.,* 2013, 20, 1-16.

26. J. Wijmans, J. Kant, M. Mulder and C. Smolders, *Polymer*, 1985, 26, 1539-1545.

27. M. Mulder, J. O. Hendrikman, J. Wijmans and C. Smolders, *J. Appl. Polym. Sci.*, 1985, 30, 2805-2820.

28. H. Bokhorst, F. Altena and C. Smolders, *Desalination.*, 1981, 38, 349-360.

29. A. Reuvers, J. Van den Berg and C. Smolders, *J. Membr. Sci.*, 1987, 34, 45-65.

30. R. Boom, I. Wienk, T. Van den Boomgaard and C. Smolders, *J. Membr. Sci.*, 1992, 73, 277-292.

31. Y. Su, C. Kuo, D. Wang, J. Lai, A. Deratani, C. Pochat and D. Bouyer, *J. Membr. Sci.*, 2009, 338, 17-28.

32. C. Kuo, H. Tsai, J. Lai, D. Wang, A. Deratani, C. Pochat-Bohatier and H. Matsuyama, *ICOM, Seoul, South Korea*, 2005.

33. J. Tsai, Y. Su, D. Wang, J. Kuo, J. Lai and A. Deratani, *J. Membr. Sci.*, 2010, 362, 360-373.

34. C. Smolders, A. Reuvers, R. Boom and I. Wienk, *Journal of Membrane Science*, 1992, 73, 259-275.

35. R. Matz, *Desalination.*, 1972, 10, 1-15.

36. M. A. Frommer and D. Lancet, in *Reverse Osmosis Membrane Research*, Springer, 1972, pp. 85-110.

37. H. Strathmann, K. Kock, P. Amar and R. Baker, *Desalination.*, 1975, 16, 179-203.

38. R. J. Ray, W. B. Krantz and R. L. Sani, *J. Membr. Sci.*, 1985, 23, 155-182.

39. M. Pekny, J. Zartman, A. Greenberg, W. Krantz and P. Todd, *Polymer Preprints, 2000,* 41 (1): 1060.

40. Č. Stropnik and V. Kaiser, *Desalination.*, 2002, 145, 1-10.

41. J. Ren, Z. Li and F.-S. Wong, *J. Membr. Sci.*, 2004, 241, 305-314.

42. V. P. Khare, A. R. Greenberg, J. Zartman, W. B. Krantz and P. Todd, *Desalination.*, 2002, 145, 17-23.

43. M. R. Pekny, J. Zartman, W. B. Krantz, A. R. Greenberg and P. Todd, *J. Membr. Sci.*, 2003, 211, 71-90.

44. H. Lee, W. B. Krantz and S.-T. Hwang, *J. Membr. Sci.*, 2010, 354, 74-85.

45. T.-H. Young, L.-P. Cheng, D.-J. Lin, L. Fane and W.-Y. Chuang, *Polymer*, 1999, 40, 5315-5323.

46. V. A. Kosma and K. G. Beltsios, *J. Membr. Sci.*, 2012, 407, 93-107.

47. R. Kumar, A. M. Isloor, A. Ismail, S. A. Rashid and T. Matsuura, *RSC Adv.*, 2013, 3, 7855-7861.

48. M. Kumar and M. Ulbricht, *RSC Adv.*, 2013, 3, 12190-12203.

49. R. J. Gohari, E. Halakoo, W. Lau, M. Kassim, T. Matsuura and A. Ismail, *RSC Adv.*, 2014, 4, 17587-17596.

50. M. A. Frommer and R. M. Messalem, *Industrial & Engineering Chemistry Product*

Research and Development, 1973, 12, 328-333.

51. Y. Pouliot, M. Wijers, S. Gauthier and L. Nadeau, *J. Membr. Sci.*, 1999, 158, 105-114.

52. M. Jerabek, Z. Major and R. Lang, *Polym. Test.*, 2010, 29, 302-309.

53. P. Meakin, *Fractals, scaling and growth far from equilibrium*, Cambridge university press, 1998.

54. M. Bikel, I. Pünt, R. Lammertink and M. Wessling, *J. Membr. Sci.*, 2010, 347, 141-149.

55. P. Van de Witte, P. Dijkstra, J. Van den Berg and J. Feijen, *J. Membr. Sci.*, 1996, 117, 1-31.

56. R. Datta, S. Dechapanichkul, J. Kim and L. Fang, *J. Membr. Sci.*, 1992, 75, 245-263.

57. S. S. Prakash, L. F. Francis and L. Scriven, *J. Membr. Sci.*, 2008, 313, 135-157.

58. S. Zereshki, A. Figoli, S. Madaeni, S. Simone, J. Jansen, M. Esmailinezhad and E. Drioli, *J. Membr. Sci.*, 2010, 362, 105-112.

59. Y. Wan, Q. Wu, S. Wang, S. Zhang and Z. Hu, *Macromol. Mater. Eng.*, 2007, 292, 598-607.

Graphical Abstract

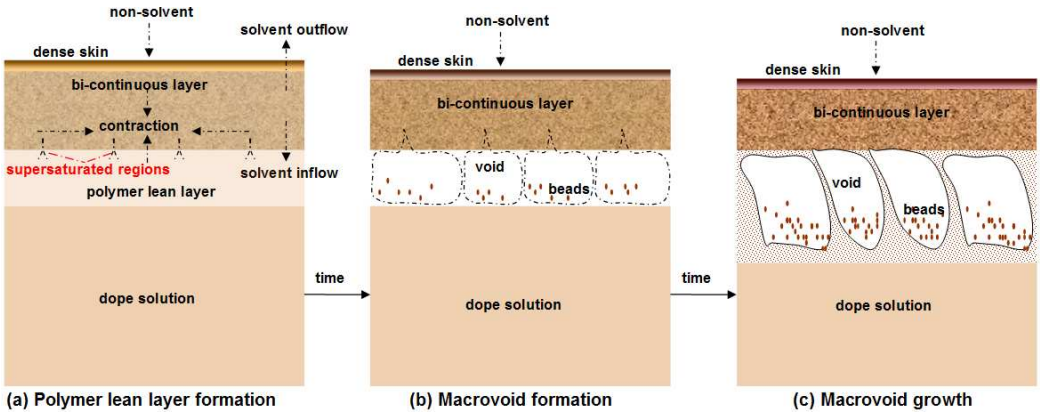

(a) Polymer lean layer formation (b) Macrovoid formation (c) Macrovoid growth